

PROTOCOL

Open Access



An end-to-end workflow to study newly synthesized mRNA following rapid protein depletion in *Saccharomyces cerevisiae*

John B. Ridenour^{1*} and Rafal Donczew^{1,2*}

Abstract

Background Gene transcription by RNA polymerase II is a fundamental process in eukaryotic cells. The precise regulation of transcription is necessary for cellular growth and development and requires the coordinated activity of numerous proteins and protein complexes. Although significant progress has been made in understanding the mechanisms that regulate transcription, many questions remain unresolved. Accurately defining the direct effects of transcriptional regulators is critical to addressing these questions. An effective approach for identifying the direct targets of transcriptional regulators is combining rapid protein depletion and quantification of newly synthesized RNA. The auxin-inducible degron (AID) system and thiol (SH)-linked alkylation for the metabolic sequencing of RNA (SLAM-seq) are powerful methods to rapidly degrade a target protein and directly quantify newly synthesized RNA, respectively. Both methods have been widely applied to study transcriptional regulation. To address unresolved questions in transcription, we assembled an end-to-end workflow to deplete proteins of interest using the AID system and measure newly synthesized RNA using SLAM-seq in the model eukaryote, *Saccharomyces cerevisiae*.

Methods We provide an open-source, step-by-step protocol to support the rapid implementation of this workflow. We include methods for targeted protein degradation, 4-thiouracil (4tU) incorporation, rapid methanol fixation, RNA purification, RNA alkylation, 3' mRNA-seq library construction, and data analysis. Additionally, we demonstrate that this workflow can help define the direct effects of transcriptional regulators using the bromodomain and extra-terminal domain (BET) proteins, Bdf1 and Bdf2, as an example.

Discussion We demonstrate that data generated using this workflow effectively quantifies 4tU-labeled transcripts and is robust to normalization using whole-cell spike-in or, at least in the case of Bdf1 and Bdf2 depletion, total read counts. We additionally demonstrate that this data correlates well with 4tU-seq data and identifies extensive differential expression due to the depletion of Bdf1 and Bdf2. Lastly, the workflow is modular and readily adaptable to other systems. Taken together, this workflow and supporting protocol will help address outstanding questions underlying the molecular basis of transcriptional regulation and other processes in *S. cerevisiae* and other eukaryotes.

Keywords *Saccharomyces cerevisiae*, Yeast, Transcription, BET proteins, Targeted protein degradation, Auxin-inducible degron system, Newly synthesized RNA, 4-thiouracil, SLAM-seq

*Correspondence:

John B. Ridenour

John-Ridenour@omrf.org

Rafal Donczew

Rafal-Donczew@omrf.org

Full list of author information is available at the end of the article



© The Author(s) 2024. **Open Access** This article is licensed under a Creative Commons Attribution 4.0 International License, which permits use, sharing, adaptation, distribution and reproduction in any medium or format, as long as you give appropriate credit to the original author(s) and the source, provide a link to the Creative Commons licence, and indicate if changes were made. The images or other third party material in this article are included in the article's Creative Commons licence, unless indicated otherwise in a credit line to the material. If material is not included in the article's Creative Commons licence and your intended use is not permitted by statutory regulation or exceeds the permitted use, you will need to obtain permission directly from the copyright holder. To view a copy of this licence, visit <http://creativecommons.org/licenses/by/4.0/>.

Background

Gene transcription by RNA polymerase II (Pol II) is a fundamental process in eukaryotic cells. The precise regulation of transcription is necessary for cellular growth and development and requires the coordinated activity of numerous proteins and protein complexes [1, 2]. For example, Pol II alone cannot initiate transcription but must cooperate with a large set of general transcription factors (GTFs), including TFIIA, TFIIB, TFIID, TFIIE, TFIIIF, and TFIIH, to perform this essential function [2, 3]. In addition to GTFs and other basal factors, sequence-specific transcription factors, transcriptional coactivators, chromatin modifiers, and chromatin remodeling factors have critical roles in regulating transcription in response to developmental or environmental cues [1, 4–6]. Despite considerable progress in understanding the molecular basis of transcriptional regulation, many questions remain unanswered. The budding yeast *Saccharomyces cerevisiae* remains an excellent system for addressing unresolved questions in transcription, as the underlying biology is broadly conserved across eukaryotes.

Defining the direct effects of transcriptional regulators is critical for elucidating their function [7, 8]. Rapid and specific degradation of target proteins is a powerful approach for identifying the direct targets of transcriptional regulators. The auxin-inducible degron (AID) system is one method for rapid protein degradation widely used to study transcriptional regulation in eukaryotes, including *S. cerevisiae* [8–13]. Derived from a plant-specific module of the conserved eukaryotic SKP1-CUL1-F-box (SCF) E3 ubiquitin ligase complex, the AID system requires the expression of the plant F-box protein TIR1 and the genetic fusion of an AID tag to a target protein to function outside of plants [11]. The addition of the plant hormone auxin promotes the association of TIR1 with the AID tag, recruitment of endogenous SCF complex components, and degradation of the target protein via the 26S proteasome. Unlike most classical genetic approaches, essential genes or synthetic lethal interactions can be studied using the AID system. We and others have used the AID system to achieve specific degradation of transcription factors, transcriptional coactivators, chromatin modifiers, and chromatin remodeling factors in *S. cerevisiae* [10, 12–16].

RNA synthesized immediately following a perturbation, such as rapid protein degradation, more accurately reflects the direct effects of the target factor than steady-state RNA [7, 8, 17]. Several sequencing-based methods selectively quantify nascent or newly synthesized RNA (reviewed in [18, 19]). These methods use various strategies to track nascent or newly synthesized RNA including the isolation of RNA associated with chromatin [20, 21], Pol II (e.g., NET-seq and mNET-seq) [22, 23], or transcriptionally competent Pol II (e.g., PRO-seq and ChRO-seq)

[24, 25] or the isolation of metabolically labeled RNA (e.g., 4sU-seq, cDTA-seq, and TT-seq) [26–28]. We and others have used 4sU-seq and the equivalent method 4tU-seq to quantify newly synthesized RNA following targeted protein depletion in *S. cerevisiae* [10, 14, 29–31]. 4sU-seq and 4tU-seq involve labeling newly synthesized RNA with 4-thiouridine (4sU) or 4-thiouracil (4tU), followed by biochemical purification of labeled RNA [10, 26, 32, 33]. Alternatively, methods such as SLAM-seq, TUC-seq, and TimeLapse-seq avoid biochemical purification by directly quantifying 4sU- or 4tU-labeled RNA following chemical recoding [7, 34–37]. In SLAM-seq, total RNA is treated with the thiol-reactive alkylating reagent iodoacetamide, which chemically recodes 4sU- or 4tU-labeled RNA and results in the misincorporation of guanosine during reverse transcription. Thus, thymine-to-cytosine (T>C) conversions define newly synthesized RNA and are quantified using dedicated data analysis software (e.g., SLAM-DUNK or GRAND-SLAM) or alternative approaches [38–41]. SLAM-seq has several advantages compared to 4tU-seq, including increased reproducibility as the purification of labeled RNA is not required. Additionally, since SLAM-seq captures both labeled and unlabeled RNA, read counts derived from newly transcribed RNA can be normalized by total read counts (i.e., the sum of reads derived from labeled and unlabeled RNA) under the assumption that steady-state RNA levels do not change considerably during a given perturbation, as is frequently the case. Thus, SLAM-seq can circumvent the need for external spike-in normalization even when global changes in transcription are observed [8, 42, 43]. Newly synthesized RNA represents only a small fraction of the total RNA pool. As such, a potential limitation of SLAM-seq compared to 4tU-seq is a decreased detection of very lowly expressed transcripts, although this limitation can be partially bypassed through increased sequencing depth. SLAM-seq and a version of cDTA-seq using iodoacetamide-mediated alkylation of labeled RNA have been applied to *S. cerevisiae*, largely to study the synthesis and decay of RNA [16, 38, 44].

Here, we provide an end-to-end workflow for rapidly degrading a target protein using the AID system and quantifying newly synthesized mRNA using SLAM-seq in *S. cerevisiae*. We include methods for targeted protein degradation, 4tU incorporation, rapid methanol fixation, RNA purification, RNA alkylation, 3' mRNA-seq library construction, and data analysis. Although the individual methods described here are not novel per se, this workflow provides the first complete resource for turnkey implementation of these methods, which will benefit others working with *S. cerevisiae*. Additionally, the modular structure allows individual methods to be replaced or removed based on user preference alleviating some

limitations to implementing the workflow. Lastly, this workflow is readily adaptable to other systems, including industrial, pathogenic, or other model fungi, and will benefit the larger research community.

Materials and procedure

The protocol described in this peer-reviewed article is published on protocols.io, updated May 31, 2024, <https://doi.org/10.17504/protocols.io.n2bvj3dj5lk5/v4>. Additional experimental details critical for generating results presented in this article are described below.

Strains and culturing conditions

Saccharomyces cerevisiae and *Schizosaccharomyces pombe* strains used in this study are listed in Table 1. Strain RDY234 was engineered using standard methods and validated using PCR and western blotting (data not shown). *Saccharomyces cerevisiae* was grown in 40 ml of YPD medium (10 g/l yeast extract, 20 g/l peptone, 20 g/l glucose, 20 mg/ml adenine sulfate) at 30 °C with shaking at 220 rpm. Cultures were grown to an OD600 of ~0.45 and split into three 10 ml cultures. Following brief equilibration, cultures were treated with 1 mM 3-indoleacetic acid (IAA) freshly prepared in dimethyl sulfoxide (DMSO) or an equivalent volume of DMSO, vigorously mixed, and incubated for 25 min at 30 °C with shaking at 220 rpm. Immediately after IAA treatment, cultures were treated with 5 mM 4tU freshly prepared in DMSO or an equivalent volume of DMSO, vigorously mixed, and incubated for 4 min at 30 °C with shaking at 220 rpm. Immediately after 4tU treatment, each culture was decanted into 5 ml of cold 100% methanol on dry ice. The resulting slurry was gently mixed by swirling to ensure homogenization and kept on dry ice. An aliquot of the slurry was collected for cell counting and western blotting. The remaining slurry was centrifuged at 3,000 g and 4 °C for 10 min to pellet the cells. Cells were resuspended in DNA/RNA shield (Zymo Research, Irvine, CA, USA) by pipetting, flash frozen on dry ice, and stored at -80 °C. The final OD600 of *S. cerevisiae* cultures was ~0.7. *Schizosaccharomyces pombe* was grown in YE medium (5 g/l yeast extract, 30 g/l glucose) at 30 °C with shaking at 220 rpm to a final OD600 of ~1.0. A

similar strategy as described for *S. cerevisiae* was used for 4tU labeling and rapid fixation of *S. pombe* cultures. For whole-cell spike-in, *S. pombe* cells were combined with *S. cerevisiae* cells in a mass-to-mass ratio of 1:19 based on OD600. Three biological replicates were collected in all experiments.

RNA alkylation and 3' mRNA-sequencing library construction

RNA alkylation was performed as previously described [7, 16] with minor modifications. A total of 5 µg of total RNA in 20 µl of nuclease-free water was used for alkylation. 3' mRNA-sequencing library construction is based on previously described methods with modifications [45, 46]. A total of 200 ng of alkylated RNA in 5 µl of nuclease-free water was used for library construction. The remaining steps of RNA alkylation and library construction are provided in detail in the full protocol. Libraries were sequenced on a NovaSeq 6000 (Illumina, San Diego, CA, USA) at the Oklahoma Medical Research Foundation (OMRF) Clinical Genomics Center (Oklahoma City, OK, USA).

Data analysis

Demultiplexed, paired-end 150 bp reads were preprocessed using fastp (version 0.23.2) [47] to extract unique molecular identifiers (UMIs) and bbdup from the BBMap package (version 39.06) (<https://sourceforge.net/projects/bbmap/>) to trim adapter sequences and polyA tails. The quality of raw and preprocessed data was assessed using FastQC (version 0.12.1) (<https://www.bioinformatics.babraham.ac.uk/projects/fastqc/>) and complied using MultiQC (version 1.21) [48]. When required, read depth was adjusted by random subsampling using SeqKit2 (version 2.0.1) [49, 50]. Forward reads were processed using SLAM-DUNK (version 0.4.3) [40]. Reads were aligned against the *S. cerevisiae* genome (version R64-3-1) or the *S. pombe* genome (version ASM294v2) using NextGenMap (version 0.5.5) [51] and single-nucleotide polymorphisms (SNPs) were called using VarScan 2 (version 2.4.5) [52] within SLAM-DUNK. Total read counts were defined as all reads remaining after alignment filtering and recovery of multimapping reads in SLAM-DUNK (Additional file 1B). Unless otherwise

Table 1 *Saccharomyces cerevisiae* and *Schizosaccharomyces pombe* strains used in this study

Strain	Species	Relevant genotype	Reference
RDY73	<i>S. cerevisiae</i>	<i>pGPD1-OsTIR1::HIS3 BDF2-3XV5-mAID-kanMX BDF1-3XV5-mAID-URA3</i>	Donczew and Hahn [10]
RDY234	<i>S. cerevisiae</i>	<i>pGPD1-OsTIR1::HIS3 BDF2-3XV5-mAID-kanMX BDF1-3XV5-mAID-URA3 pBDF1-BDF1::TRP1</i>	This study
SHY1058	<i>S. pombe</i>	<i>RPB3-3XFLAG-natMX</i>	Warfield et al. [13]

indicated, a conversion per read threshold of ≥ 2 T>C conversions was used to define T>C read counts (Additional file 1C). Data analysis is described in detail in the full protocol.

To define counting windows in SLAM-DUNK, custom BED files were created for both *S. cerevisiae* and *S. pombe*. Open reading frames (ORFs) were extracted from the *S. cerevisiae* annotation (version R64-3-1) or the *S. pombe* annotation (version ASM294v2) using BEDOPS (version 2.4.3). Preliminary analyses demonstrated that reads aligned to gene bodies and 3' untranslated regions (UTRs) (data not shown). Therefore, all ORFs were extended 250 bp beyond their stop position to include 3' UTRs using SAMtools (version 1.14) and BEDTools (version 2.30.0). Custom BED files were deposited in the Zenodo repository (<https://doi.org/10.5281/zenodo.10714018>). Chromosome names were modified in the *S. cerevisiae* reference files (i.e., genome assembly and BED file) to reflect standard nomenclature [53].

Spike-in normalization factors were calculated as the sum of all *S. pombe* read counts (T>C read counts and non-T>C read counts) divided by 1×10^5 (Additional file 1D). The factor 1×10^5 was arbitrarily chosen to ensure spike-in normalization factors were between one and ten. Total counts normalization factors were calculated as the sum of all *S. cerevisiae* read counts (T>C read counts and non-T>C read counts) divided by 1×10^6 (Additional file 1D). The factor 1×10^6 was arbitrarily chosen to ensure total counts normalization factors were between one and ten. Normalization and differential gene expression analysis were performed on raw data (total read counts or T>C read counts) using DESeq2 (version 1.38.3) [54]. Adjusted *p*-values were calculated with independent hypothesis weighting using IHW (version 1.26.0) [55] within DESeq2. Genes classified as dubious open reading frames (ORFs) or pseudogenes or that did not meet criteria for fold change and/or *p*-value calculations in DESeq2 were excluded from subsequent analyses. The remaining genes were filtered against 5313 genes previously found to be reliably detected under experimental conditions comparable to those used in this study [10], leaving 5311 genes. To compare SLAM-seq and 4tU-seq data, genes were further filtered against 4883 genes that were previously found to provide high reproducibility and low information loss in 4tU-seq experiments with strain RDY73 [10], leaving 4882 genes. For strict filtering, dubious ORFs and pseudogenes were removed. The remaining genes were filtered on the requirement of having ≥ 1 T>C read count across all samples. Data processing and plotting were performed using R (version 4.2.3) (<https://www.R-project.org/>) and RStudio (version 2023.12.0 + 369) (<http://www.rstudio.com/>).

General notes and troubleshooting

In the protocol described here, newly transcribed RNA is metabolically labeled with 4tU. Both *S. cerevisiae* and *S. pombe* readily import 4tU without genetic manipulation or specific media requirements [56–58]. Although not a requirement, previous studies suggest that in certain contexts the expression of an additional copy of endogenous uridine or uracil permeases (Fui1 and Fur4, respectively) or depletion of uracil in growth media can improve 4tU incorporation in *S. cerevisiae* [33]. Previous studies also suggest that brief exposure to 4tU at low concentrations, such as the conditions used in this protocol, has minimal effects on the growth of *S. cerevisiae* [56, 57], although high concentrations or prolonged exposure can be detrimental. Relatedly, the auxin, IAA, is used in the described protocol to induce protein depletion via an AID system. While IAA is known to affect aspects of *S. cerevisiae* biology [59, 60], relatively short exposure to IAA at low concentrations is generally considered to have minimal effects. As previously suggested, the optimal conditions for IAA treatment (e.g., time, concentration) should be empirically determined to minimize off-target effects [61]. It should also be noted that low levels of depletion in the absence of exogenous IAA have been reported for some target proteins [62, 63]. Modified AID systems, such as the β -est AID, super-sensitive AID, or AID2 systems [62–64], may reduce off-target effects and, as more data emerges for the use of these systems in *S. cerevisiae*, may improve this protocol.

A key step in SLAM-seq is the alkylation of a uracil analog (i.e., 4sU or 4tU) incorporated into RNA using iodoacetamide [7, 44]. We note that iodoacetamide is unstable and light sensitive. Therefore, iodoacetamide should be prepared immediately before use and protected from light [7]. Additionally, alkylation reactions should be performed in the dark and simultaneously on all samples within an experiment when possible. We and others [8] provide data that a conversion per read threshold of ≥ 2 T>C conversions effectively reduces background signal. However, we recommend that initial SLAM-seq experiments include an untreated (i.e., -4tU) control to assess spurious nucleotide conversions and polymorphisms between experimental and reference strains. SLAM-seq quantifies both steady-state (non-T>C read counts) and newly transcribed RNA (T>C read counts) simultaneously [7, 40]. Newly transcribed RNA is a small fraction of the total. Similar to what others have demonstrated [8, 38], we present evidence that SLAM-seq data can be normalized using exogenous whole cell spike-in or total read counts (i.e., the sum of T>C read counts and non-T>C read counts). However, the proposed total read counts normalization strategy is specific for data derived from

SLAM-seq and related methods (e.g., TimeLapse-seq). Additionally, although this strategy works well for our example case (Bdf1/2 depletion), it does not supplant spike-in normalization, and we recommend initially testing total counts normalization in parallel with spike-in normalization for different target proteins and/or experimental conditions.

Methods that use a template switching oligo (TSO) for constructing sequencing libraries, such as that described here, often generate forward reads that start with three low-diversity bases. It is therefore necessary to increase the diversity of the library pool when sequencing on an Illumina instrument. A final library pool should contain 10–15% libraries constructed using standard approaches [65] or a control library (e.g., PhiX Control v3; Illumina) (see Veeranagouda et al. [45] for additional details). Third, the method for constructing mRNA-seq libraries described here supports barcoding in the forward and reverse reads, although like many 3' mRNA-seq methods (e.g., QuantSeq FWD; Lexogen, Greenland, NH, USA) the reverse read is generally of low quality and provides little information beyond barcoding. In our experience, paired-end sequencing is more cost-effective than single-end sequencing at many service providers. We also note that the number of recovered T>C read counts is dependent on read length, for example, more T>C read counts per gene recovered from 150 bp reads compared to 100 bp reads at an equivalent read depth (data not shown). Therefore, together with data presented here, we recommend sequencing 5 to 10 million paired-end 150 bp reads per sample depending on the goals of an experiment.

Lastly, we anticipate this workflow will be readily adapted to other systems. Although we acknowledge that some optimization will be necessary depending on the system, our data from spike-in, 4tU-labeled *S. pombe* cells suggests this workflow can be directly applied to *S. pombe*. Additionally, using parts of the workflow without modification, we have successfully prepared alkylated RNA and 3' mRNA-seq libraries using 4sU-labeled total RNA derived from human cell lines (data not shown).

Expected results

Applying the SLAM-seq workflow to study transcriptional regulation in *Saccharomyces cerevisiae*

To illustrate expected results, we performed experiments with two *S. cerevisiae* strains (RDY73 and RDY234) related to our studies on BET proteins. BET (bromodomain and extra-terminal domain) proteins are conserved chromatin readers characterized by two bromodomains and an extra-terminal (ET) domain [66]. BET proteins have an integral role in transcriptional regulation, although the

mechanisms by which they regulate transcription are not well understood [10, 66–68]. There are two BET proteins (Bdf1 and Bdf2, referred to here as Bdf1/2) in *S. cerevisiae*, and deletion of both *BDF1* and *BDF2* is lethal [69]. Although Bdf1 and Bdf2 have overlapping functions, the depletion of Bdf1 has a more significant impact on global transcription [10]. Strain RDY73 carries a codon-optimized *Oryza sativa* TIR1 protein (OsTIR1) [11] and mAID-tagged Bdf1/2 and was previously used to study changes in transcription after depletion of Bdf1/2 [10]. The mAID (miniAID) is a codon-optimized minimum region (65–132 aa) of the *Arabidopsis thaliana* IAA17 protein [70, 71]. To obtain strain RDY234, an additional, unmodified copy of *BDF1* driven by its endogenous promoter was integrated at the *TRP1* locus in strain RDY73.

In this study, cells of strain RDY73 or RDY234 in the logarithmic phase were treated with the auxin 3-indoleacetic acid (IAA) for 25 min to deplete Bdf1/2 then treated with 4-thiouracil (4tU) for 4 min to label newly synthesized RNA. Immediately after 4tU labeling, cells were rapidly fixed in cold methanol on dry ice as described [33, 72–74]. It was previously demonstrated that within this timeframe IAA treatment resulted in more than a 90% reduction in the level of Bdf1 and an approximately 85% reduction in the level of Bdf2 [10]. We observed a similar depletion of Bdf1/2 by western blotting (data not shown). Subsequently, RNA was purified, alkylated, reverse transcribed, and sequenced. The resulting data was processed using SLAM-DUNK. All experiments were performed in biological triplicate.

To assess how well our workflow quantifies 4tU-labeled transcripts, we first calculated percent conversion rates in reads mapped to defined windows. We observed a strong and specific accumulation of T>C conversions in 4tU-treated cells compared to untreated cells (Fig. 1A–B). Second, we calculated percent read counts with zero, one, or ≥ 2 T>C conversions mapped to defined windows. We observed that most reads have zero T>C conversions in both 4tU-treated and untreated cells and that, although a percentage of reads with one T>C conversion in untreated cells was observed, 4tU-treated cells have a much higher percentage of reads with one or ≥ 2 T>C conversions compared to untreated cells (Fig. 1C–D). We also calculated the percent background signal in reads with ≥ 1 or 2 T>C conversions mapped to defined windows. Here, we observed a substantially lower percent background signal in reads with ≥ 2 T>C conversions compared to reads with ≥ 1 T>C conversions (Fig. 1E). Together, these results illustrate that our workflow can selectively quantify 4tU-labeled transcripts and that counting reads with ≥ 2 T>C conversions effectively reduces background signal.

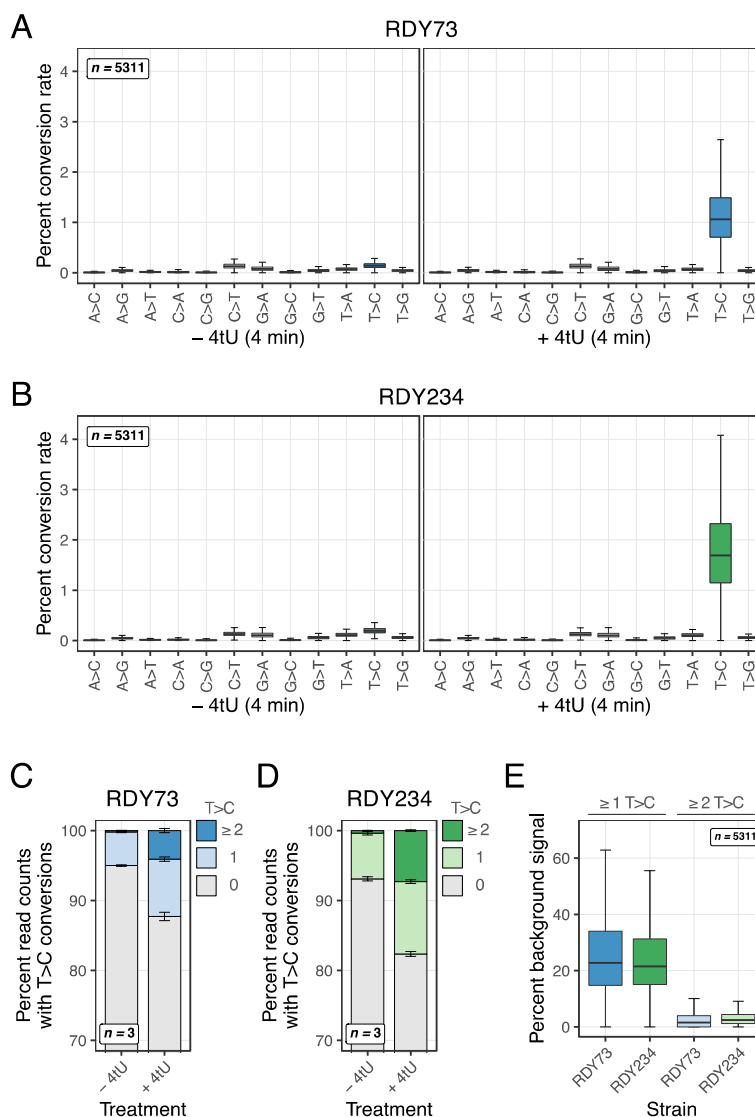


Fig. 1 Application of SLAM-seq to *Saccharomyces cerevisiae*. **A** Boxplots comparing percent conversion rates in reads mapped to defined windows. SLAM-seq data was derived from strain RDY73 treated with (+) or without (-) 4-thiouracil (4tU) for 4 min. Mean conversion rates for three biological replicates across the indicated number of transcripts ($n = 5311$) are presented as Tukey boxplots. Outliers are not shown. **B** Boxplots comparing percent conversion rates in reads mapped to defined windows. SLAM-seq data was derived from strain RDY234 treated with (+) or without (-) 4tU for 4 min. Mean conversion rates for three biological replicates across the indicated number of transcripts ($n = 5311$) are presented as Tukey boxplots. Outliers are not shown. **C** Barplots comparing percent read counts with 0, 1, or ≥ 2 T>C conversions mapped to defined windows. SLAM-seq data was derived from strain RDY73 treated with (+) or without (-) 4tU for 4 min. Mean values for biological replicates ($n = 3$) are plotted. Error bars represent the standard deviation of the mean. The y-axis begins at 70 percent. **D** Barplots comparing percent read counts with 0, 1, or ≥ 2 T>C conversions mapped to defined windows. SLAM-seq data was derived from strain RDY234 treated with (+) or without (-) 4tU for 4 min. Mean values for biological replicates ($n = 3$) are plotted. Error bars represent the standard deviation of the mean. The y-axis begins at 70 percent. **E** Boxplots comparing percent background signal in reads with ≥ 1 or ≥ 2 T>C conversions mapped to defined windows. SLAM-seq data was derived from strains RDY73 or RDY234 treated with (+) or without (-) 4tU for 4 min. Mean background signals for three biological replicates across the indicated number of transcripts ($n = 5311$) are presented as Tukey boxplots. Outliers are not shown

SLAM-seq detects global transcriptional changes associated with rapid depletion of Bdf1/2 and is robust to normalization using whole-cell spike-in or total read counts

Normalization by whole-cell spike-in

In SLAM-seq experiments, we performed whole-cell spike-in normalization using 4tU-labeled *S. pombe* cells as previously described [10, 14]. Here, we calculated

spike-in normalization factors based on *S. pombe* total read counts. We then used the spike-in normalization factors to normalize (1) total read counts or (2) T > C read counts in DESeq2 (Additional file 1E-G). Interestingly, we observed a global loss of transcription following Bdf1/2 depletion for both spike-in normalized total read counts and spike-in normalized T > C read counts derived from strain RDY73 (Fig. 2A-B). These results

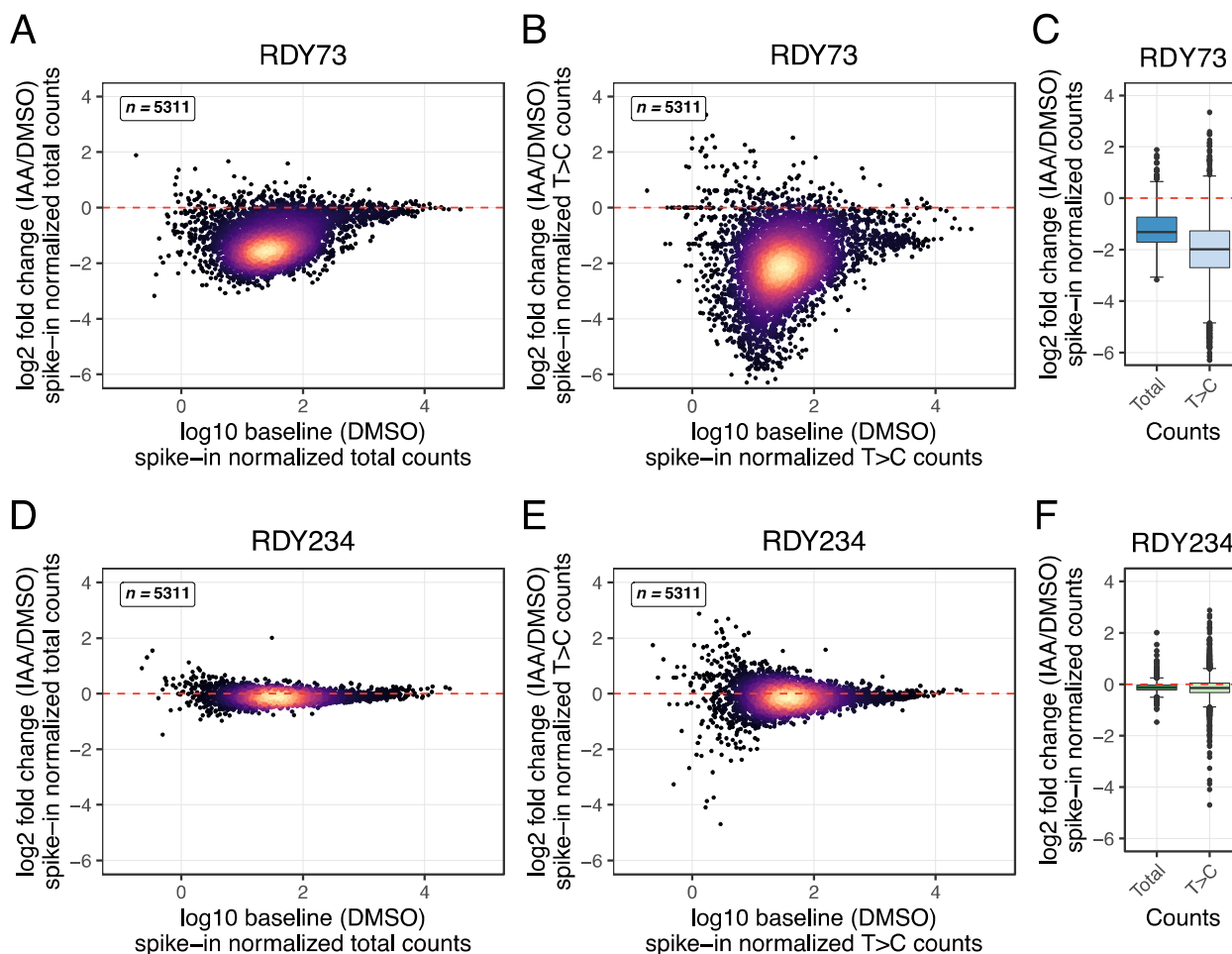


Fig. 2 SLAM-seq detects global transcriptional changes associated with rapid depletion of Bdf1/2. **A** Scatterplot comparing log₂ fold change in transcription and log₁₀ baseline transcription following Bdf1/2 depletion (strain RDY73) across the indicated number of transcripts ($n = 5311$). Total read counts were normalized using size factors calculated on total read counts from exogenous whole cell spike-in. Mean values for three biological replicates are plotted. **B** Scatterplot comparing log₂ fold change in transcription and log₁₀ baseline transcription following Bdf1/2 depletion (strain RDY73) across the indicated number of transcripts ($n = 5311$). T > C read counts were normalized using size factors calculated on total read counts from exogenous whole cell spike-in. Mean values for three biological replicates are plotted. **C** Boxplots comparing log₂ fold changes in transcription following Bdf1/2 depletion (strain RDY73) normalized using exogenous whole cell spike-in. Mean changes in transcription for three biological replicates across 5311 transcripts are presented as Tukey boxplots. **D** Scatterplot comparing log₂ fold change in transcription and log₁₀ baseline transcription following Bdf1/2 depletion in a strain ectopically expressing *BDF1* (RDY234) across the indicated number of transcripts ($n = 5311$). Total read counts were normalized using size factors calculated on total read counts from exogenous whole cell spike-in. Mean values for three biological replicates are plotted. **E** Scatterplot comparing log₂ fold change in transcription and log₁₀ baseline transcription following Bdf1/2 depletion in a strain ectopically expressing *BDF1* (RDY234) across the indicated number of transcripts ($n = 5311$). T > C read counts were normalized using size factors calculated on total read counts from exogenous whole cell spike-in. Mean values for three biological replicates are plotted. **F** Boxplots comparing log₂ fold changes in transcription following Bdf1/2 depletion in a strain ectopically expressing *BDF1* (RDY234) normalized using exogenous whole cell spike-in. Mean changes in transcription for three biological replicates across 5311 transcripts are presented as Tukey boxplots

indicate that substantial changes in transcription are already apparent in steady-state RNA 30 min after inducing Bdf1/2 depletion. However, the magnitude of the transcriptional changes is much more dramatic in newly synthesized RNA compared to steady-state RNA (Fig. 2C). We did not observe global changes in transcription for either spike-in normalized total read counts or spike-in normalized T>C read counts derived from strain RDY234 (Fig. 2D-F), indicating that ectopically expressed *BDF1* largely complements depletion of endogenous Bdf1/2. Together, these results illustrate the importance of measuring newly synthesized RNA to study the direct effects of a perturbation such as rapid protein depletion.

We additionally tested normalization using *S. pombe* reads with ≥ 2 T>C conversions rather than total *S. pombe* reads, though no substantial benefit was found using this approach (data not shown). However, as a general consideration, we note that 4tU-labeled spike-in may be needed to control for alkylation efficiency if samples within an experimental set are independently treated with iodoacetamide or if samples will also be used for methods that rely on the enrichment of labeled RNA (e.g., 4tU-seq or TT-SLAM-seq [14, 75]).

Normalization by total read counts

In previous studies, SLAM-seq data has been normalized using total read counts rather than whole-cell spike-in [8, 42, 43]. These studies demonstrated that normalizing T>C read count data by total read count data is a robust approach even when global changes in transcription are observed. A similar normalization strategy has also been proposed for TimeLapse-seq data [36]. In addition, potential issues with spike-in normalization have been noted [76, 77]. Therefore, we tested a normalization approach using total read counts to circumvent the need for whole-cell spike-in and streamline our workflow.

Previous studies used DESeq2 to calculate size factors based on total read counts. Total read counts were defined as the sum of T>C read counts and non-T>C read counts following alignment and filtering. The DESeq2 size factors were then used to normalize T>C read counts. We initially applied this approach to data derived from strain RDY73. We observed a global loss of transcription following Bdf1/2 depletion for DESeq2 normalized T>C read counts (Fig. 3A). However, the magnitude of these changes was less than what we observed for spike-in normalized T>C read counts (Fig. 2B). The median-ratio method implemented by DESeq2 to estimate size factors assumes that the expression of most genes is not affected by

experimental conditions [54]. However, previous work has demonstrated that depletion of Bdf1/2 results in global changes in newly transcribed mRNA [10]. Here, we demonstrate that depletion of Bdf1/2 results in substantial changes in steady-state mRNA within 30 min (Fig. 2A). Thus, we presume that the extent to which Bdf1/2 depletion affects newly transcribed and steady-state mRNA violates assumptions underlying DESeq2 calculations and that, although DESeq2 size factors (calculated on total read counts) can be used to effectively normalize SLAM-seq data in certain contexts (i.e., mammalian cells), this approach does not recapitulate the results we observed using exogenous whole cell spike-in (Fig. 2B). Although not tested in this study, we note that other strategies for calculating size factors can be implemented in DESeq2, such as calculating size factors on a subset of control genes expected to be stably expressed across all samples in a given experiment.

Based on these results, we reasoned that an alternative normalization approach using total read counts might yield better results for a rapidly dividing organism like *S. cerevisiae*. Thus, we calculated normalization factors based on total read counts for each sample (see Materials and Procedure). We then used these total counts normalization factors to normalize T>C read counts in DESeq2 (Additional file 1H-I). Using this approach, we again observed a global loss of transcription following Bdf1/2 depletion (Fig. 3B). However, the magnitude of transcriptional changes was more dramatic when T>C read counts were normalized by total counts normalization factors compared to DESeq2 size factors. This was more apparent when DESeq2 or total counts normalized T>C read counts were compared to spike-in normalized T>C read counts (Fig. 3C-D). Notably, only a minimal shift in read counts per gene was observed for total counts normalized T>C read counts compared to spike-in normalized T>C read counts (Fig. 3D). Together, these results illustrate that SLAM-seq data derived from *S. cerevisiae* can be reliably normalized using normalization factors derived from total read counts.

SLAM-seq correlates well with 4tU-seq and identifies extensive differential expression following depletion of Bdf1/2

Next, we compared our SLAM-seq data (spike-in or total counts normalized T>C read counts) to published 4tU-seq data derived from strain RDY73 under comparable experimental conditions [10]. A striking loss of transcription is apparent in the data from both SLAM-seq (Fig. 2B; Fig. 3B) and 4tU-seq [10].

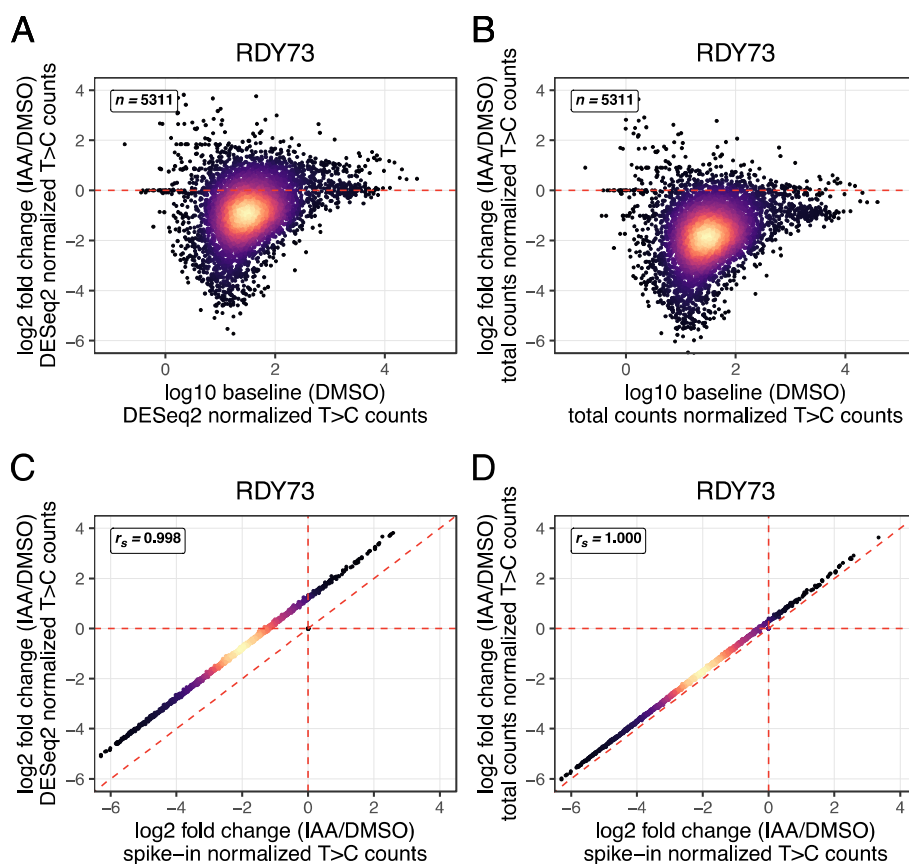


Fig. 3 SLAM-seq is robust to normalization using total read counts. **A** Scatterplot comparing log₂ fold change in transcription and log₁₀ baseline transcription following Bdf1/2 depletion across the indicated number of transcripts ($n = 5311$). T>C read counts were normalized using size factors estimated on total read counts using DESeq2. Mean values for three biological replicates are plotted. **B** Scatterplot comparing log₂ fold change in transcription and log₁₀ baseline transcription following Bdf1/2 depletion across the indicated number of transcripts ($n = 5311$). T>C read counts were normalized using size factors calculated on total read counts. Mean values for three biological replicates are plotted. **C** Scatterplot comparing log₂ fold change in transcription following Bdf1/2 depletion determined across 5311 transcripts. T>C read counts were normalized using size factors estimated on total read counts using DESeq2 or normalized using size factors calculated on total read counts from exogenous whole cell spike-in. Spearman's correlation coefficient (r_s) is shown. **D** Scatterplot comparing log₂ fold change in transcription following Bdf1/2 depletion determined across 5311 transcripts. T>C read counts were normalized size factors calculated on total read counts or size factors calculated on total read counts from exogenous whole cell spike-in. Spearman's correlation coefficient (r_s) is shown

Comparing the change in transcription across the two datasets, we observe a strong correlation between SLAM-seq and 4tU-seq data (Fig. 4A and C). Furthermore, we observed extensive differential expression following Bdf1/2 depletion (Fig. 4B). For example, we detected six upregulated genes and 3425 downregulated genes for spike-in normalized T>C read counts using a false discovery rate (FDR) adjusted p -value ≤ 0.05 and log₂ fold change $\geq |1|$ as cutoffs (Fig. 4B). Additionally, we detected eight upregulated genes and 2622 downregulated genes for total counts normalized T>C read counts using the same cutoffs (Fig. 4D). Together, these results illustrate a strong correlation between SLAM-seq and 4tU-seq data and

demonstrate that our workflow can help define the direct targets of transcriptional regulators such as Bdf1/2 using either spike-in or total counts normalization strategies.

Lastly, we compared how the number of genes recovered by SLAM-seq correlates with read depth. Here, we randomly subsampled SLAM-seq data derived from strain RDY73. After processing subsampled data using SLAM-DUNK, we calculated spike-in normalization factors based on *S. pombe* total read counts and used the spike-in normalization factors to normalize T>C read counts in DESeq2. Results were then filtered using relaxed or strict criteria (see Materials and Procedure). Unsurprisingly, the number of genes we could reliably quantify

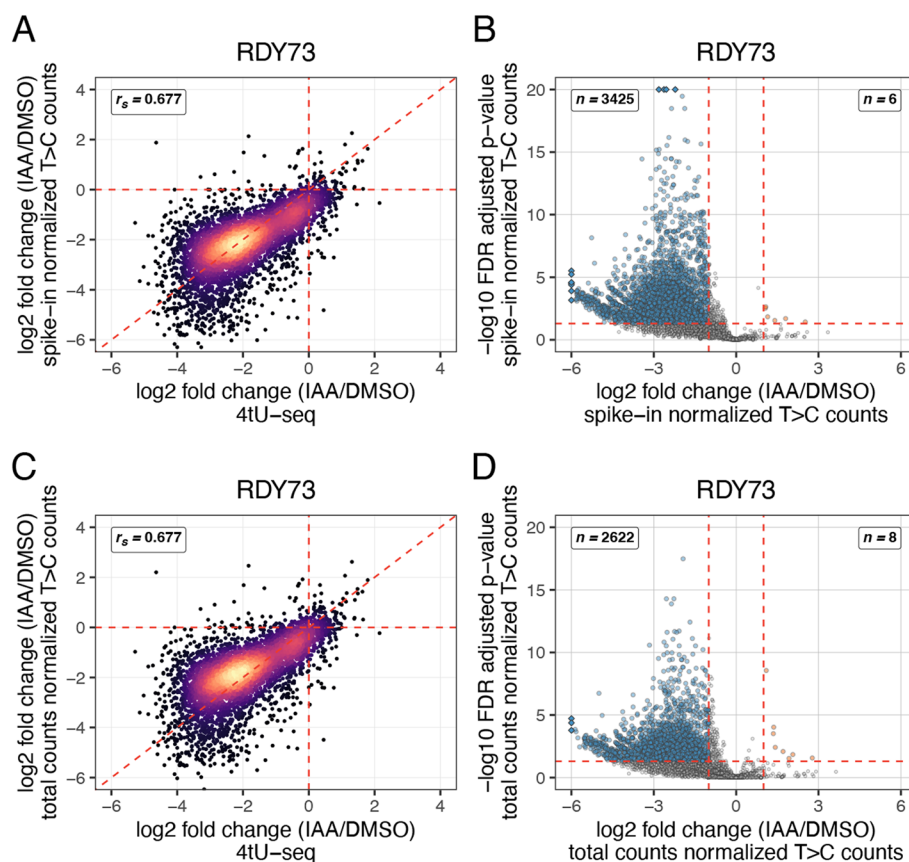


Fig. 4 SLAM-seq correlates well with 4tU-seq and identifies extensive differential expression following Bdf1/2 depletion. **A** Scatterplot comparing log₂ fold change in transcription following Bdf1/2 depletion determined using SLAM-seq or 4tU-seq across 4882 transcripts. T > C read counts derived from SLAM-seq were normalized using size factors calculated on total read counts from exogenous whole cell spike-in. Mean values for three biological replicates are plotted. Read counts derived from previously published 4tU-seq data were normalized using size factors calculated on total read counts from exogenous whole cell spike-in. Spearman's correlation coefficient (r_s) is shown. **B** Volcano plot comparing $-\log_{10}$ false discovery rate (FDR) adjusted p -value and log₂ fold change in transcription following Bdf1/2 depletion across 5311 transcripts. T > C read counts were normalized using size factors calculated on total read counts from exogenous whole cell spike-in. Mean values for three biological replicates are plotted. Differentially expressed genes are defined using an FDR adjusted p -value ≤ 0.05 and log₂ fold change $\geq |1|$ as cutoffs. Numbers of differentially expressed genes are shown in respective regions of the plot. **C** Scatterplot comparing log₂ fold change in transcription following Bdf1/2 depletion determined using SLAM-seq or 4tU-seq across 4882 transcripts. T > C read counts derived from SLAM-seq were normalized size factors calculated on total read counts. Mean values for three biological replicates are plotted. Read counts derived from previously published 4tU-seq data were normalized using size factors calculated on total read counts from exogenous whole cell spike-in. Spearman's correlation coefficient (r_s) is shown. **D** Volcano plot comparing $-\log_{10}$ false discovery rate (FDR) adjusted p -value and log₂ fold change in transcription following Bdf1/2 depletion across 5311 transcripts. T > C read counts were normalized using size factors calculated on total read counts. Mean values for three biological replicates are plotted. Differentially expressed genes are defined using an FDR adjusted p -value ≤ 0.05 and log₂ fold change $\geq |1|$ as cutoffs. Numbers of differentially expressed genes are shown in respective regions of the plot

decreased with read depth, which was most apparent when “strict” filtering was applied (Fig. 5). However, these results demonstrate that our workflow recovers a substantial number of protein-coding genes. For example, when we subsampled 5.5 million reads per sample, we recovered 5273 genes using “relaxed” filtering criteria and 3428 genes using “strict” filtering criteria, representing approximately 87 percent or 57 percent of protein-coding genes, respectively (Fig. 5; Additional file 1).

Conclusions

We provide an end-to-end workflow for rapid and specific protein degradation using the AID system and selective quantification of newly synthesized RNA using SLAM-seq in *S. cerevisiae*. The workflow builds on established methods to provide a complete resource for implementation. We demonstrate that the workflow can help define the direct effects of transcriptional regulators using the BET proteins Bdf1/2 as an example. Together, this workflow will help address outstanding questions

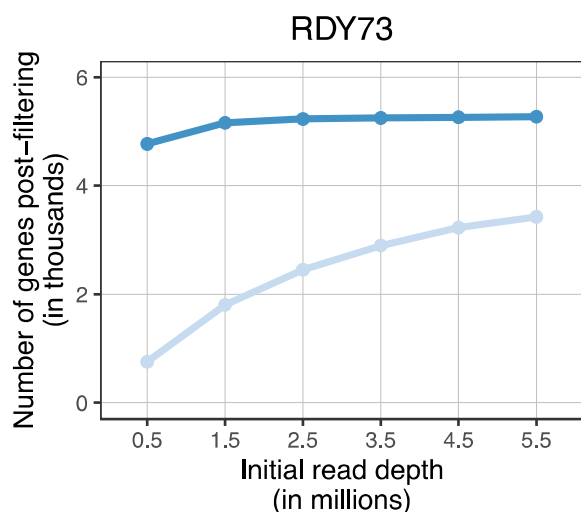


Fig. 5 The number of genes recovered by SLAM-seq correlates with read depth. Lineplot comparing the number of genes recovered post-filtering and initial read depth. SLAM-seq data was derived from strain RDY73 treated with 4-thiouracil (4tU) for 4 min. T > C read counts were normalized using size factors calculated on total read counts from exogenous whole cell spike-in. Genes were filtered as described in Materials and Procedure (relaxed filtering; dark blue line) or on the requirement that genes have \geq one T > C read count across all samples ($n=6$) (strict filtering; light blue line). Genes classified as dubious open reading frames (ORFs) or pseudogenes were removed in both filtering procedures. To adjust initial read depth, reads were randomly subsampled prior to SLAM-DUNK processing (see Materials and Procedure)

underlying the molecular basis of transcription and other biological processes in *S. cerevisiae*. In addition, this workflow is readily adaptable to other systems and will benefit the larger research community.

Abbreviations

AID	Auxin-inducible degron
BET	Bromodomain and extra-terminal domain
DMSO	Dimethyl sulfoxide
DTT	Dithiothreitol
FDR	False discovery rate
4sU	4-Thiouridine
4tU	4-Thiouracil
GTF	General transcription factors
IAA	3-Indoleacetic acid
ORF	Open reading frame
Pol II	RNA polymerase II
SLAM-seq	Thiol (SH)-linked alkylation for the metabolic sequencing of RNA
T > C	Thymine-to-cytosine
TSO	Template switching oligo
UTR	Untranslated region

Supplementary Information

The online version contains supplementary material available at <https://doi.org/10.1186/s44330-024-00008-1>.

Supplementary Material 1.

Acknowledgements

We thank Magdalena Donczew for assistance in generating genetic resources and Magdalena Donczew and Agnieszka Machowska for helpful discussion and critically reviewing the protocol and manuscript. We thank the OMRF Research Computing Services, Clinical Genomics Center, and Center for Biomedical Data Sciences for key contributions to the work described in this manuscript. We thank Steven Hahn for sharing the *Saccharomyces cerevisiae* and *Schizosaccharomyces pombe* strains RDY73 and SHY1058.

Authors' contributions

JBR and RD conceptualized and designed the protocol. JBR performed the experiments. JBR and RD analyzed and interpreted the data. JBR and RD wrote the protocol and manuscript. JBR and RD read and approved the final manuscript.

Funding

This work was supported by institutional startup funds provided by OMRF to RD.

Availability of data and materials

SLAM-seq data were deposited in the NCBI Gene Expression Omnibus (GEO) database under accession number GSE261145 and are additionally accessible from the NCBI Sequence Read Archive (SRA) under BioProject PRJNA1085387. The reference genome assemblies and annotations for *Saccharomyces cerevisiae* strain S288C (version R64-3-1, RefSeq Assembly GCF_000146045.2) and *Schizosaccharomyces pombe* strain 972h- (version ASM294v2, RefSeq Assembly GCF_000002945.1) were retrieved from the NCBI Datasets repository. Published 4tU-seq data (GEO Dataset GSE171067) were retrieved from the NCBI GEO repository. All other relevant data supporting key findings in this study are available within the article or available from the corresponding authors upon request.

Declarations

Ethics approval and consent to participate

Not applicable.

Consent for publication

Not applicable.

Competing interests

The authors declare no competing interests.

Author details

¹Cell Cycle and Cancer Biology Research Program, Oklahoma Medical Research Foundation, Oklahoma City, OK, USA. ²Department of Cell Biology, University of Oklahoma Health Sciences Center, Oklahoma City, OK, USA.

Received: 20 March 2024 Accepted: 4 July 2024

Published online: 11 July 2024

References

- Hahn S. Structure and mechanism of the RNA polymerase II transcription machinery. *Nat Struct Mol Biol.* 2004;11:394–403.
- Schier AC, Taatjes DJ. Structure and mechanism of the RNA polymerase II transcription machinery. *Genes Dev.* 2020;34:465–88.
- Malik S, Roeder RG. Regulation of the RNA polymerase II pre-initiation complex by its associated coactivators. *Nat Rev Genet.* 2023;24:767–82.
- Mellor J. The dynamics of chromatin remodeling at promoters. *Mol Cell.* 2005;19:147–57.
- Richter WF, Nayak S, Iwasa J, Taatjes DJ. The mediator complex as a master regulator of transcription by RNA polymerase II. *Nat Rev Mol Cell Biol.* 2022;23:732–49.
- Spitz F, Furlong EEM. Transcription factors: from enhancer binding to developmental control. *Nat Rev Genet.* 2012;13:613–26.
- Herzog VA, Reichholf B, Neumann T, Rescheneder P, Bhat P, Burkard TR, et al. Thiol-linked alkylation of RNA to assess expression dynamics. *Nat Methods.* 2017;14:1198–204.

8. Muhar M, Ebert A, Neumann T, Umkehrer C, Jude J, Wieshofer C, et al. SLAM-seq defines direct gene-regulatory functions of the BRD4-MYC axis. *Science*. 2018;360:800–5.
9. Barrass JD, Mendoza-Ochoa GI, Maudlin IE, Sani E, Beggs JD. Tuning Degradation to Achieve Specific and Efficient Protein Depletion. *JoVE (J Vis Exp)*. 2019;149:e59874.
10. Donczew R, Hahn S. BET family members Bdf1/2 modulate global transcription initiation and elongation in *Saccharomyces cerevisiae*. *eLife*. 2021;10:e69619.
11. Nishimura K, Fukagawa T, Takisawa H, Kakimoto T, Kanemaki M. An auxin-based degron system for the rapid depletion of proteins in nonplant cells. *Nat Methods*. 2009;6:917–22.
12. Warfield L, Donczew R, Mahendrawada L, Hahn S. Yeast mediator facilitates transcription initiation at most promoters via a tail-independent mechanism. *Mol Cell*. 2022;82:4033–4048.e7.
13. Warfield L, Ramachandran S, Baptista T, Devys D, Tora L, Hahn S. Transcription of nearly all yeast RNA polymerase II-transcribed genes is dependent on transcription factor TFIID. *Mol Cell*. 2017;68:118–129.e5.
14. Donczew R, Warfield L, Pacheco D, Erijman A, Hahn S. Two roles for the yeast transcription coactivator SAGA and a set of genes redundantly regulated by TFIID and SAGA. *eLife*. 2020;9:e50109.
15. Ellison MA, Namjilsuren S, Shirra MK, Blacksmith MS, Schusteff RA, Kerr EM, et al. Spt6 directly interacts with Cdc73 and is required for Paf1 complex occupancy at active genes in *Saccharomyces cerevisiae*. *Nucleic Acids Res*. 2023;51:4814–30.
16. Klein-Brill A, Joseph-Strauss D, Appleboim A, Friedman N. Dynamics of chromatin and transcription during transient depletion of the RSC chromatin remodeling complex. *Cell Rep*. 2019;26:279–292.e5.
17. Jaeger MG, Winter GE. Fast-acting chemical tools to delineate causality in transcriptional control. *Mol Cell*. 2021;81:1617–30.
18. Duffy EE, Schofield JA, Simon MD. Gaining insight into transcriptome-wide RNA population dynamics through the chemistry of 4-thiouridine. *WIREs RNA*. 2019;10:e1513.
19. Wissink EM, Vihervaara A, Tippens ND, Lis JT. Nascent RNA analyses: tracking transcription and its regulation. *Nat Rev Genet*. 2019;20:705–23.
20. Henikoff S, Henikoff JG, Sakai A, Loeb GB, Ahmad K. Genome-wide profiling of salt fractions maps physical properties of chromatin. *Genome Res*. 2009;19:460–9.
21. Mayer A, di Iulio J, Maleri S, Eser U, Vierstra J, Reynolds A, et al. Native elongating transcript sequencing reveals human transcriptional activity at nucleotide resolution. *Cell*. 2015;161:541–54.
22. Churchman LS, Weissman JS. Nascent transcript sequencing visualizes transcription at nucleotide resolution. *Nature*. 2011;469:368–73.
23. Schlackow M, Nojima T, Gomes T, Dhir A, Carmo-Fonseca M, Proudfoot NJ. Distinctive patterns of transcription and RNA processing for human lincRNAs. *Mol Cell*. 2017;65:25–38.
24. Kwak H, Fuda NJ, Core LJ, Lis JT. Precise maps of RNA polymerase reveal how promoters direct initiation and pausing. *Science*. 2013;339:950–3.
25. Chu T, Rice EJ, Booth GT, Salamanca HH, Wang Z, Core LJ, et al. Chromatin run-on and sequencing maps the transcriptional regulatory landscape of glioblastoma multiforme. *Nat Genet*. 2018;50:1553–64.
26. Duffy EE, Rutenber-Schoenberg M, Stark CD, Kitchen RR, Gerstein MB, Simon MD. Tracking distinct RNA populations using efficient and reversible covalent chemistry. *Mol Cell*. 2015;59:858–66.
27. Rodríguez-Molina JB, Tseng SC, Simonett SP, Taunton J, Ansari AZ. Engineered covalent inactivation of TFIIF-kinase reveals an elongation checkpoint and results in widespread mRNA stabilization. *Mol Cell*. 2016;63:433–44.
28. Schwab B, Michel M, Zacher B, Frühauf K, Demel C, Tresch A, et al. TT-seq maps the human transient transcriptome. *Science*. 2016;352:1225–8.
29. Baptista T, Grünberg S, Minoungou N, Koster MJE, Timmers HTM, Hahn S, et al. SAGA is a general cofactor for RNA polymerase II transcription. *Mol Cell*. 2017;68:130–143.e5.
30. Mahendrawada L, Warfield L, Donczew R, Hahn S. Surprising connections between DNA binding and function for the near-complete set of yeast transcription factors. *bioRxiv*. 2023:2023.07.25.550593.
31. Saleh MM, Jeronimo C, Robert F, Zentner GE. Connection of core and tail mediator modules restrains transcription from TFIID-dependent promoters. *PLoS Genet*. 2021;17:e1009529.
32. Baptista T, Devys D. *Saccharomyces cerevisiae* metabolic labeling with 4-thiouracil and the quantification of newly synthesized mRNA as a proxy for RNA polymerase II activity. *JoVE (J Vis Exp)*. 2018;140:57982.
33. Barrass JD, Beggs JD. Extremely rapid and specific metabolic labelling of RNA in vivo with 4-thiouracil (Ers4tU). *JoVE (J Vis Exp)*. 2019;150:59952.
34. Riml C, Amort T, Rieder D, Gasser C, Lusser A, Micura R. Osmium-mediated transformation of 4-thiouridine to cytidine as key to study RNA dynamics by sequencing. *Angew Chem Int Ed*. 2017;56:13479–83.
35. Matsushima W, Herzog VA, Neumann T, Gapp K, Zuber J, Ameres SL, et al. SLAM-ITseq: sequencing cell type-specific transcriptomes without cell sorting. *Development*. 2018;145:dev164640.
36. Schofield JA, Duffy EE, Kiefer L, Sullivan MC, Simon MD. TimeLapse-seq: adding a temporal dimension to RNA sequencing through nucleoside recoding. *Nat Methods*. 2018;15:221–5.
37. Lusser A, Gasser C, Trixl L, Piatti P, Delazer I, Rieder D, et al. Thiouridine-to-Cytidine Conversion Sequencing (TUC-Seq) to measure mRNA transcription and degradation rates. In: LaCava J, Vaňáčová Š, editors., et al., *The eukaryotic RNA exosome: methods and protocols*. New York, NY: Springer; 2020. p. 191–211.
38. Chappeboim A, Joseph-Strauss D, Gershon O, Friedman N. Transcription feedback dynamics in the wake of cytoplasmic mRNA degradation shutdown. *Nucleic Acids Res*. 2022;50:5864–80.
39. Jürges C, Dölken L, Erhard F. Dissecting newly transcribed and old RNA using GRAND-SLAM. *Bioinformatics*. 2018;34:218–26.
40. Neumann T, Herzog VA, Muhar M, Von Haeseler A, Zuber J, Ameres SL, et al. Quantification of experimentally induced nucleotide conversions in high-throughput sequencing datasets. *BMC Bioinformatics*. 2019;20:258.
41. Rummel T, Sakellaridi L, Erhard F. grandR: a comprehensive package for nucleotide conversion RNA-seq data analysis. *Nat Commun*. 2023;14:3559.
42. Aksenova V, Smith A, Lee H, Bhat P, Esnault C, Chen S, et al. Nucleoporin TPR is an integral component of the TREX-2 mRNA export pathway. *Nat Commun*. 2020;11:4577.
43. Wang H, Fan Z, Shliaha PV, Miele M, Hendrickson RC, Jiang X, et al. H3K4me3 regulates RNA polymerase II promoter-proximal pause-release. *Nature*. 2023;615:339–48.
44. Alalam H, Zepeda-Martínez JA, Sunnerhagen P. Global SLAM-seq for accurate mRNA decay determination and identification of NMD targets. *RNA*. 2022;28:905–15.
45. Veeranagouda Y, Remaury A, Guillemot J-C, Didier M. RNA Fragmentation and Sequencing (RF-Seq): cost-effective, time-efficient, and high-throughput 3' mRNA sequencing library construction in a single tube. *Curr Protoc Mol Biol*. 2019;129:e109.
46. Foley JW, Zhu C, Jolivet P, Zhu SX, Lu P, Meaney MJ, et al. Gene-expression profiling of single cells from archival tissue with laser-capture microdissection and Smart-3SEQ. *Genome Res*. 2019;29:1816–25.
47. Chen S, Zhou Y, Chen Y, Gu J. fastp: an ultra-fast all-in-one FASTQ pre-processor. *Bioinformatics*. 2018;34:i884–90.
48. Ewels P, Magnusson M, Lundin S, Käller M. MultiQC: summarize analysis results for multiple tools and samples in a single report. *Bioinformatics*. 2016;32:3047–8.
49. Shen W, Le S, Li Y, Hu F. SeqKit: a cross-platform and ultrafast toolkit for FASTA/Q file manipulation. *PLoS ONE*. 2016;11:e0163962.
50. Shen W, Sipsos B, Zhao L. SeqKit2: A Swiss army knife for sequence and alignment processing. *iMeta*. 2024;3:e191.
51. Sedlazeck FJ, Rescheneder P, von Haeseler A. NextGenMap: fast and accurate read mapping in highly polymorphic genomes. *Bioinformatics*. 2013;29:2790–1.
52. Koboldt DC, Zhang Q, Larson DE, Shen D, McLellan MD, Lin L, et al. VarScan 2: Somatic mutation and copy number alteration discovery in cancer by exome sequencing. *Genome Res*. 2012;22:568–76.
53. Engel SR, Dietrich FS, Fisk DG, Binkley G, Balakrishnan R, Costanzo MC, et al. The reference genome sequence of *Saccharomyces cerevisiae*: then and now. *G3 (Bethesda)*. 2013;4:389–98.
54. Love MI, Huber W, Anders S. Moderated estimation of fold change and dispersion for RNA-seq data with DESeq2. *Genome Biol*. 2014;15:550.
55. Ignatiadis N, Huber W. Covariate powered cross-weighted multiple testing. *J R Stat Soc Ser B Stat Methodol*. 2021;83:720–51.

56. Munchel SE, Shultzaberger RK, Takizawa N, Weis K. Dynamic profiling of mRNA turnover reveals gene-specific and system-wide regulation of mRNA decay. *MBoC*. 2011;22:2787–95.
57. Sun M, Schwalb B, Schulz D, Pirkl N, Etzold S, Larivière L, et al. Comparative dynamic transcriptome analysis (cDTA) reveals mutual feedback between mRNA synthesis and degradation. *Genome Res*. 2012;22:1350–9.
58. Eser P, Wachutka L, Maier KC, Demel C, Boroni M, Iyer S, et al. Determinants of RNA metabolism in the *Schizosaccharomyces pombe* genome. *Mol Syst Biol*. 2016;12:857.
59. Nicastro R, Raucci S, Michel AH, Stumpe M, Osuna GMG, Jaquenoud M, et al. Indole-3-acetic acid is a physiological inhibitor of TORC1 in yeast. *PLoS Genet*. 2021;17:e1009414.
60. Domeni Zali G, Moriel-Carretero M. Auxin alone provokes retention of ASH1 mRNA in *Saccharomyces cerevisiae* mother cells. *MicroPubl Biol*. 2023. <https://doi.org/10.17912/micropub.biology.000752>.
61. Shetty A, Reim NI, Winston F. Auxin-inducible degron system for depletion of proteins in *Saccharomyces cerevisiae*. *Curr Protoc Mol Biol*. 2019;128:e104.
62. Mendoza-Ochoa GI, Barrass JD, Terlouw BR, Maudlin IE, de Lucas S, Sani E, et al. A fast and tuneable auxin-inducible degron for depletion of target proteins in budding yeast. *Yeast*. 2019;36:75–81.
63. Yesbolatova A, Saito Y, Kitamoto N, Makino-Itou H, Ajima R, Nakano R, et al. The auxin-inducible degron 2 technology provides sharp degradation control in yeast, mammalian cells, and mice. *Nat Commun*. 2020;11:5701.
64. Nishimura K, Yamada R, Hagihara S, Iwasaki R, Uchida N, Kamura T, et al. A super-sensitive auxin-inducible degron system with an engineered auxin-TIR1 pair. *Nucleic Acids Res*. 2020;48:e108.
65. Möller M, Ridenour JB, Wright DF, Martin FA, Freitag M. H4K20me3 is important for Ash1-mediated H3K36me3 and transcriptional silencing in facultative heterochromatin in a fungal pathogen. *PLoS Genet*. 2023;19:e1010945.
66. Eischer N, Arnold M, Mayer A. Emerging roles of BET proteins in transcription and co-transcriptional RNA processing. *WIREs RNA*. 2023;14:e1734.
67. Gaub A, Sheikh BN, Basilicata MF, Vincent M, Nizon M, Colson C, et al. Evolutionary conserved NSL complex/BRD4 axis controls transcription activation via histone acetylation. *Nat Commun*. 2020;11:2243.
68. Winter GE, Mayer A, Buckley DL, Erb MA, Roderick JE, Vittori S, et al. BET Bromodomain proteins function as master transcription elongation factors independent of CDK9 recruitment. *Mol Cell*. 2017;67:5–18.e19.
69. Matangasombut O, Buratowski RM, Swilling NW, Buratowski S. Bromodomain factor 1 corresponds to a missing piece of yeast TFIIID. *Genes Dev*. 2000;14:951–62.
70. Kubota T, Nishimura K, Kanemaki MT, Donaldson AD. The Elg1 replication factor c-like complex functions in PCNA unloading during DNA replication. *Mol Cell*. 2013;50:273–80.
71. Nishimura K, Kanemaki MT. Rapid depletion of budding yeast proteins via the fusion of an Auxin-Inducible Degron (AID). *Curr Protoc Cell Biol*. 2014;64:20.9.1–16.
72. Alexander RD, Barrass JD, Dichtl B, Kos M, Obtulowicz T, Robert M-C, et al. RiboSys, a high-resolution, quantitative approach to measure the in vivo kinetics of pre-mRNA splicing and 3'-end processing in *Saccharomyces cerevisiae*. *RNA*. 2010;16:2570–80.
73. Aslanzadeh V, Huang Y, Sanguinetti G, Beggs JD. Transcription rate strongly affects splicing fidelity and cotranscriptionality in budding yeast. *Genome Res*. 2018;28:203–13.
74. Barrass JD, Reid JEA, Huang Y, Hector RD, Sanguinetti G, Beggs JD, et al. Transcriptome-wide RNA processing kinetics revealed using extremely short 4tU labeling. *Genome Biol*. 2015;16:282.
75. Reichholf B, Herzog VA, Fasching N, Manzenreither RA, Sowemimo I, Ameres SL. Time-resolved small RNA sequencing unravels the molecular principles of MicroRNA homeostasis. *Mol Cell*. 2019;75:756–768.e7.
76. Risso D, Ngai J, Speed TP, Dudoit S. Normalization of RNA-seq data using factor analysis of control genes or samples. *Nat Biotechnol*. 2014;32:896–902.
77. Robinson MD, Oshlack A. A scaling normalization method for differential expression analysis of RNA-seq data. *Genome Biol*. 2010;11:R25.

Publisher's Note

Springer Nature remains neutral with regard to jurisdictional claims in published maps and institutional affiliations.